

Nonlinear renormalization of electromagnetic wave spectra in metals: the anomalous doppleron

V. A. Burdov and V. Ya. Demikhovskii

N. I. Lobachevskii Gorki State University

(Received 28 February 1991)

Zh. Eksp. Teor. Fiz. **100**, 647–661 (August 1991)

The spectral renormalization of electromagnetic waves of finite amplitude propagating in metals is investigated. The change in nondissipative conductivity attributable to the nonlinear nature of particle motion in the wave field is found. A qualitative analysis is carried out and equations of motion of electrons with an arbitrary spectrum $\varepsilon(\mathbf{p})$ in a uniform magnetic field \mathbf{B}_0 and a circularly-polarized wave field are found. The spectral renormalization effects of an electron doppleron in cadmium are examined. Such effects are manifested as a reduction in the period of surface impedance oscillations and a shift of these oscillations toward stronger fields \mathbf{B}_0 with increasing wave amplitude. The nonlinear effects are shown to be sensitive to the behavior of the portion of the electronic spectrum responsible for the threshold conductivity (the intersection with the extremal value of the derivative $\partial S/\partial p_z$ or the reference point). These effects are compared to experimental results.³

1. INTRODUCTION

The interaction between a strong electromagnetic wave and resonant electrons may have a significant effect on the conductivity of a metal. This interaction will principally reduce the dissipative part of the conductivity and cause a corresponding decrease in nondissipative damping, since it is the resonant particles that make the primary contribution to the damping. Moreover, the interaction of charged particles with a wave will also modify the nondissipative part of the conductivity, which leads to renormalization of the real part of the spectrum. Since, as a rule, all particles—not just the resonant ones—contribute to the nondissipative conductivity, the nonlinear renormalization effects of the real part of the spectrum will generally be less strongly expressed than the nonlinear damping effects.

The nonlinear spectral renormalization problem was first analyzed by Morales and O'Neil¹ in a study of longitudinal plasma waves. The nonlinear frequency shift $\delta\omega$ was shown to asymptotically (as $t \rightarrow \infty$) approach a quantity proportional to the oscillation frequency of the trapped particles $\bar{\omega}$. Karpman and Lundin² calculated the nonlinear frequency shift of circularly polarized waves (whistlers) propagating in a gaseous plasma.

The present paper is devoted to an investigation of the effects of nonlinear renormalization of the spectrum of electromagnetic waves propagating in a degenerate electron-hole metal plasma. The nature of this problem is such that, as a rule, we have an essentially nonquadratic energy spectrum of the carriers $\varepsilon(\mathbf{p})$ and, moreover, the degeneration of the electron-hole plasma yields a discernible collisionless cyclotron absorption threshold.

The real and imaginary parts of the conductivity are, as a rule, nonanalytic at the threshold, with the character of the singularity determined by the electronic spectrum at the reference point or near the intersection of the Fermi surface with the extremal value of the derivative $\partial S/\partial p_z$ (S is the cross section of the Fermi surface and p_z is the projection of the momentum in the direction of the magnetic field). As suggested in this study, the dispersion law of the electromag-

netic wave will change most significantly with increasing wave amplitude near the absorption threshold due to the effect of the wave on particles either near the reference point or at the intersection with the extremal of $\partial S/\partial p_z$. It will be demonstrated, specifically, that the strong nonlinear renormalization of conductivity (both the real and imaginary parts) may generate waves of a new type beyond the collisionless absorption threshold. Such waves have been observed experimentally in cadmium and may have been detected in tungsten.³ In addition to the well-known electron doppleron propagating along the magnetic field with zero collisionless damping, a new branch of opposite polarity was also discovered beyond the collisionless cyclotron absorption threshold under nonlinear conditions in cadmium. Such anomalous dopplerons have not been observed under linear conditions.

Before solving the spectral renormalization problem, we analyze the dynamics of particles with a complex electron dispersion law in a longitudinal magnetic field \mathbf{B}_0 and in the field of a circularly-polarized electromagnetic wave traveling parallel to \mathbf{B}_0 (Sec. 2). The distribution function of the resonant electrons is then calculated by means of the kinetic Boltzmann equation (Sec. 3). The nonlinear correction to the nondissipative conductivity and the nonlinear spectral renormalization are calculated in Sec. 4. The parameters of the anomalous doppleron in cadmium observed in Ref. 3 are discussed in the final, fifth section.

2. PARTICLE DYNAMICS

Let us consider the dynamics of a charged particle in the field of a circularly polarized electromagnetic wave propagating in the direction of a fixed, uniform magnetic field \mathbf{B}_0 . We assume cylindrical symmetry of the Fermi surface of the metal, and carry out a preliminary qualitative analysis of this dynamical system for a comparatively simple model of the electronic spectrum

$$\varepsilon(p_{\perp}; p_z) = \frac{p_{\perp}^2}{2m} + \varepsilon_{\parallel}(p_z). \quad (1)$$

We write the equations of motion and analyze the phase portrait of the system. There is no electrical field associated with the wave in the coordinate system traveling with the phase velocity v_p of the wave while the magnetic field coincides with the electrical field in the laboratory frame accurate to terms of the order of $(v_p/c)^2$. In this case the initial equations of motion take the form

$$\frac{d\mathbf{p}}{dt} = -\frac{e}{c} [\mathbf{v}; \mathbf{B}_0 + \mathbf{B}], \quad (2)$$

where e is electron charge, c is the speed of light, $\mathbf{v} = \partial\epsilon/\partial\mathbf{p}$ is particle velocity, and $\mathbf{B} = (B \sin kz, B \cos kz, 0)$ is the field of the circularly-polarized wave ("—" polarization). Since the total energy of the particle $\epsilon(\mathbf{p}) - v_p p_z$ is conserved in the comoving frame, one of the equations of the system (2) can be dropped. The two remaining equations are easily written for the longitudinal momentum p_z and for the angle β between the magnetic field of the wave and the transverse velocity vector of the particle \mathbf{v}_\perp :

$$\begin{aligned} \frac{dp_z}{d\tau} &= -\hbar m v_\perp \sin \beta, \\ \frac{d\beta}{d\tau} &= 1 + kv_z/\omega_c + \hbar v_z/v_\perp \cos \beta. \end{aligned} \quad (3)$$

Here $\tau = \omega_c t$ is dimensionless time, ω_c is the cyclotron frequency, $\hbar = B/B_0$, and k is the wave vector, $\beta = \varphi + kz + \pi/2$, $\varphi = \arctg(v_y/v_x)$. The stationary points of Eqs. (3) are found by the equations

$$\sin \beta = 0, \quad \beta = \pi n, \quad (4a)$$

$$1 + kv_z/\omega_c = (-1)^{n+1} \hbar v_z(p_z)/v_\perp(p_z). \quad (4b)$$

Let us first analyze the system (4) assuming that the velocity $v_z(p)$ has no extremum in the momentum domain $-p_F < p_z < p_F$ (Fig. 1a). The position of the stationary points on the p_z axis depends on $q = kv_F/\omega_c$. This is illustrated by Fig. 2. Curves 1 and 2 represent the dependence of the left side of Eq. (4b) on p_z for different values of parameter q . Curves 3 and 4 are plots of the right side of the equation with an even (curve 3) and odd (curve 4) value of n . The intersections of these curves define the position of the stationary points on the phase plane. Figure 2 reveals that for $q < 1$ there are two stationary points in the neighborhood of $p_z = \pm p_F$. Both of these points are "centers" (see Fig. 3a). The situation changes with increasing q : curves 1 and 4 make contact and a third "saddle-center" singularity appears at a certain value $q = q_0$ (Fig. 3b). Finally there are four singularities for $q > q_0$: these are "centers" and "saddles" (Fig. 3c).

When the velocity $v_z(p_z)$ has an extremum (Fig. 1b), equations (4a) and (4b) continue to describe the position of

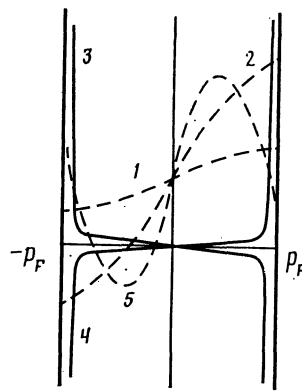
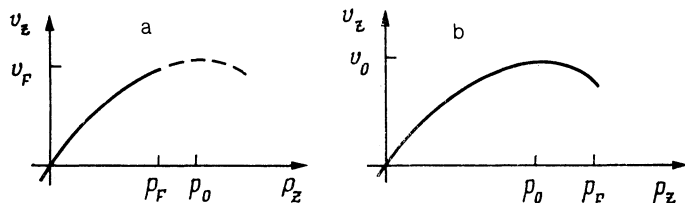


FIG. 2. Graphical solution of Eq. (4b) that determines the position of the stationary points.

the stationary points on the phase plane, although there may be an increasing number of solutions of Eq. (4b) (the number of intersections of curve 5 in Fig. 2). Specifically, there may be two cyclotron resonances symmetrical to the extremum of $v_z(p_z)$.

We now analyze the more general model of the electronic spectrum

$$\epsilon = \epsilon(p_\perp; p_z). \quad (5)$$

We represent the vector potential \mathbf{A} in a constant magnetic field parallel to the z axis and in the field of a perpendicularly polarized wave as

$$\mathbf{A} \left(\frac{B}{k} \sin(kz - \omega t); B_0 x + \frac{B}{k} \cos(kz - \omega t); 0 \right).$$

We then have for the Hamiltonian

$$H = \epsilon(p_z; p_\perp), \quad (6)$$

where

$$\begin{aligned} p_\perp^2 &= \left(p_x + \frac{eB}{ck} \sin(kz - \omega t) \right)^2 \\ &+ \frac{e^2 B_0^2}{c^2} \left(x + x_0 + \frac{\hbar}{k} \cos(kz - \omega t) \right)^2, \end{aligned}$$

ω is the frequency of the electromagnetic wave, $x_0 = cp_y/eB_0$.

We now need to carry out a number of canonical transforms on Hamiltonian (6) corresponding to a transition to the comoving frame of the wave and selection of more convenient action-angle canonically conjugate variables. These transforms are carried out in the Appendix.

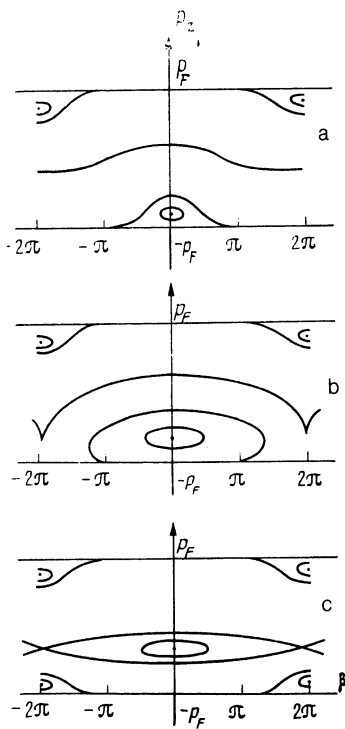


FIG. 3. Phase portraits of the dynamical system (3) for different values of the parameter q .

Particle dynamics in the vicinity of different singularities on the phase plane can be analyzed by means of equations of motion (A6) listed in the Appendix. We, however, will only focus on the neighborhood of cyclotron resonance defined in linear theory by the condition

$$kv_z(J+\mathbf{P}; \mathbf{P}) + \omega_c(J+\mathbf{P}; \mathbf{P}) = 0, \quad (7)$$

where the actions \mathbf{P} and J are given by Eqs. (A3). It is this domain, as will be demonstrated below, that makes the strongest contribution to spectral renormalization and damping of the wave.

Carrying out an expansion in the resonant shift of the momentum $s = -P_1$ defined by condition (7) in (A6), and introducing the dimensionless momentum $s = (P + P_1)/\tilde{P}$ and time $\tau = \tilde{\omega}t$, we obtain the following Hamiltonian system:

$$\begin{aligned} \frac{ds}{d\tau} &= -\frac{\partial \mathcal{H}}{\partial \beta} = -\sin \beta + vs \sin \beta, \\ \frac{d\beta}{d\tau} &= \frac{\partial \mathcal{H}}{\partial s} = s + 3\mu s^2 + v \cos \beta, \end{aligned} \quad (8)$$

$$\mathcal{H} = \frac{1}{2}s^2 - \cos \beta + \mu s^3 + vs \cos \beta.$$

Here

$$\tilde{P} = \left(h \frac{\omega_c(-P_1)p_\perp(-P_1)}{kG} \right)^{1/2},$$

$$\tilde{\omega} = \left(h \frac{\omega_c(-P_1)p_\perp(-P_1)G}{k} \right)^{1/2}$$

is the characteristic resonant width and characteristic oscillation

frequency of the trapped particles, respectively, while the parameters

$$v = \frac{\hbar}{\tilde{\omega}} \frac{\partial}{\partial P} (v_z p_\perp) |_{-P_1} \ll 1, \quad \mu = \frac{R}{3G} \tilde{P} \ll 1,$$

$$G = \frac{\partial}{\partial P} (kv_z + \omega_c)_{J, -P_1} = -\frac{k^2}{2\pi m_c} \left(\frac{\partial^2 S}{\partial p_z^2} \right)_{\varepsilon, -P_1},$$

$$\begin{aligned} R &= \frac{1}{2} \frac{\partial^2}{\partial P^2} (kv_z + \omega_c)_{J, -P_1} \\ &= \frac{1}{2} \left(-\frac{ck^3}{\pi e B_0} \frac{\partial \omega_c}{\partial p_z} \left(\frac{\partial^2 S}{\partial p_z^2} \right)_\varepsilon - \frac{k^3}{2\pi m_c} \left(\frac{\partial^3 S}{\partial p_z^3} \right)_\varepsilon \right)_{-P_1} \end{aligned}$$

are expressed through the derivatives of the resonant cross section $S(\varepsilon_F; p_z)$ and the derivative of the cyclotron frequency (m_c is the cyclotron mass).

It is possible to simplify the Hamiltonian (8) by eliminating the term $vs \cos \beta$ through the change of variables

$$s = v - v \cos \beta, \quad \beta = \beta,$$

after which, to within small terms of order v^2 and $v\mu$, we have

$$\begin{aligned} H &= v^2/2 - \cos \beta + \mu v^3, \\ \dot{v} &= -\sin \beta, \\ \dot{\beta} &= v + 3\mu v^2. \end{aligned} \quad (8a)$$

We therefore arrive at the Hamiltonian of a mathematical pendulum with an additional small parameter μv^3 . This addition will be shown to have little effect on wave damping, although it is significant in determining spectral renormalization.

3. KINETICS OF RESONANT PARTICLES

The electron distribution function of the resonant particles satisfies the kinetic Boltzmann equation, which in the comoving frame of the wave in the variables J, ϑ, P, β takes the form

$$\frac{\partial f}{\partial t} + \dot{P} \frac{\partial f}{\partial P} + \dot{\beta} \frac{\partial f}{\partial \beta} = -\frac{f - f_0}{\tau_p}, \quad (10)$$

where the collision integral is written in a relaxation-time approximation, τ_p is the drift time, $f_0(\varepsilon' + v_p p_z = \text{const})$ is the equilibrium distribution function, while $\varepsilon' = \varepsilon - v_p p_z = \text{const}$ is the energy in the comoving frame. The time dependence of the distribution function in the comoving frame is entirely attributable to the temporal dependence of the amplitude, i.e., damping, so this permits neglecting the term $\partial f / \partial t$ in Eq. (10). Assuming $f = f_0 + g$, we obtain for the nonequilibrium correction g

$$\frac{dg}{dt} + \frac{g}{\tau_p} = -\frac{df_0}{dt} = h v_p \omega_c p_\perp f'_0 \sin \beta, \quad (11)$$

where $f'_0 = df_0/d\varepsilon$.

The electron collisions in Eq. (11) must be taken into account in order to calculate the nonlinear absorption coefficient of the wave. This coefficient is found to be proportional to the nonlinearity parameter a , which in turn is equal to the ratio of the electron collision frequency τ_p^{-1} to the oscillation

tion frequency of the trapped particles $\tilde{\omega}$ (Ref. 4). Renormalization of the real part of the spectrum appears even in zeroth order in a , i.e., it has a collisionless nature. Therefore, allowing τ_p to approach infinity in Eq. (11), we obtain

$$g = -\omega f_0' \left(P - \bar{P} + \frac{\hbar}{k} (p_{\perp} \cos \beta - \overline{p_{\perp} \cos \beta}) \right), \quad (12)$$

where the prime denotes time averaging.

We have neglected the dependence of f_0' on s in Eq. (11) in calculating Eq. (12). Taking this relation into account will lead to terms proportional to f_0'' , etc. in Eq. (12). The term with f_0'' in the distribution function of Ref. 1 made the principal contribution to the frequency renormalization of a Langmuir wave propagating in a Maxwellian plasma. The frequency shift of a circularly-polarized wave in a non-degenerate plasma was determined in Ref. 2 by terms proportional to both f_0' and f_0'' . In our case terms with f_0'' are clearly small compared to the remaining terms in Eq. (12) in the parameter v_p/v_F due to Fermi degeneracy. It is easily determined that to first order in the wave amplitude the distribution function (12) becomes

$$g_L = -\hbar v_p p_{\perp} f_0' \frac{\omega_c}{k v_z + \omega_c} \cos \beta. \quad (13)$$

Writing the expression for the field-generated current by means of the distribution functions (12) and (13), we obtain the nonlinear renormalization of the Hall conductivity:

$$\Delta\sigma = \sigma_{xy} - \sigma_{xy}^L = -\frac{2ec}{(2\pi\hbar)^3 v_p B} \int d\mathbf{p} v_{\perp} \cos \beta (g - g_L). \quad (14)$$

We evaluate the momentum integral in (14) by going over to the dimensionless momentum s , phase β , and action J introduced above. Here

$$f_0' d\mathbf{p} = -k m_e \bar{P} \delta(J - J_F) dJ d\beta ds,$$

where J_F is the value of action J on the Fermi surface. It is simple to carry out the integration with respect to J , and Eq. (14) then becomes

$$\Delta\sigma = -\frac{2eck\omega_c(-P_{\perp})p_{\perp}^2(-P_{\perp})}{(2\pi\hbar)^3 GB_0} \int ds d\beta (1 + \gamma s) \cos \beta \times \left\{ s - \bar{s} - \frac{1 - \gamma s}{s + 3\mu s^2} \cos \beta - \overline{\eta \cos \beta} \right\}, \quad (15)$$

where the following dimensionless small parameters are introduced:

$$\eta = \frac{\tilde{\omega}}{\omega_c}, \quad \gamma = \left(\frac{\partial p_{\perp}}{\partial P} \right)_{J, -P, p_{\perp}(-P_{\perp})} \frac{\bar{P}}{p_{\perp}(-P_{\perp})}.$$

We then calculate \bar{s} and $\overline{\cos \beta}$ in Eq. (15). For this purpose we define v_0 as

$$v_0 = \pm (2(H + \cos \beta))^{1/2},$$

and by means of the Hamiltonian (8a) obtain the relation $v(\beta)$ with small μ :

$$v(\beta) \approx v_0 - \mu v_0^2. \quad (16)$$

We find \bar{v} by evaluating the corresponding integral over period T :

$$\bar{v} = \frac{1}{T} \int_{-\pi/2}^{\pi/2} d\tau v(H, \tau). \quad (17)$$

Evaluation of integral (17) by means of the equations of motion (8a) allowing for the small value of μ , for passing particles ($H > 1$) reduces to

$$\bar{v} = \frac{1}{T} \int_{-\pi}^{\pi} d\beta (1 - 3\mu v_0) = \omega(\kappa) \left(1 - \frac{12}{\pi} \mu \frac{\mathbf{E}(\kappa)}{\kappa} \right),$$

where $\omega(\kappa) = 2\pi/T$ is the oscillation frequency, $\mathbf{E}(\kappa)$ is a complete elliptical integral of the second kind, and the dimensionless parameter κ is given by

$$\kappa^2 = \frac{2}{H+1}.$$

We use the following approach to determine oscillation frequency $\omega(\kappa)$. We introduce the action I as

$$I = \frac{1}{2\pi} \int_{-\pi}^{\pi} v(\beta) d\beta$$

and, using the expansion (16), we obtain

$$I = \frac{4}{\pi} \frac{\mathbf{E}(\kappa)}{\kappa} - 2\mu \left(\frac{2}{\kappa^2} - 1 \right). \quad (18)$$

Now, calculating $\omega(\kappa)$ as

$$\omega(\kappa) = \frac{dH}{d\kappa} / \frac{dI}{d\kappa},$$

we finally have for the passing particles

$$\bar{v} = \frac{\pi}{\kappa \mathbf{K}(\kappa)} + 2\mu \left(\frac{\pi}{\kappa \mathbf{K}(\kappa)} \right)^2 - 12\mu \frac{\mathbf{E}(\kappa)}{\kappa^2 \mathbf{K}(\kappa)}, \quad (19)$$

where $\mathbf{K}(\kappa)$ is a complete elliptical integral of the first kind.

Carrying out analogous calculations for the trapped particles, we have

$$\bar{v} = -12\mu \frac{\mathbf{E}(\kappa^{-1}) - (1 - \kappa^{-2}) \mathbf{K}(\kappa^{-1})}{\mathbf{K}(\kappa^{-1})}. \quad (20)$$

For $\mu = 0$ Eqs. (19) and (20) become the familiar expressions obtained by approximating the Hamiltonian to be that of the mathematical pendulum.

We need only calculate $\overline{\cos \beta}$ to lowest order in μ , which yields for the passing and trapped particles

$$\overline{\cos \beta} = \frac{1}{T} \int \frac{d\beta \cos \beta}{v(\beta)} = \begin{cases} 1 + \frac{2}{\kappa^2} \left(\frac{\mathbf{E}(\kappa)}{\mathbf{K}(\kappa)} - 1 \right), & \kappa < 1, \\ \frac{2\mathbf{E}(\kappa^{-1})}{\mathbf{K}(\kappa^{-1})} - 1, & \kappa > 1, \end{cases} \quad (21)$$

respectively. We then have for \bar{s}

$$\bar{s} = \bar{v} - \nu \overline{\cos \beta},$$

where \bar{v} and $\overline{\cos \beta}$ are given by Eqs. (19), (20), and (21). This value of \bar{s} completely determines the distribution function (12) and the nonlinear correction to the nondissipative conductivity (15).

4. NONLINEAR SPECTRAL RENORMALIZATION

We now determine the nonlinear correction to the conductivity σ_{xy} and renormalization of the spectrum $\omega(k)$ by means of the linear g_L and nonlinear g distribution functions obtained in the preceding section using Eqs. (14) and (15).

We go from the variables s, β to the variables κ, β in the double integral (15), after which it is possible to integrate with respect to β . The integral with respect to the variable β is taken largely in the same manner as in Ref. 2, and we therefore need not consider its evaluation in detail here. The integration with respect to κ is carried out numerically, which yields

$$\Delta\sigma = -\frac{64e^2S(-P_1)}{(2\pi\hbar)^3k|S''(-P_1)|}(2F\mu+Q(\nu-\eta)), \quad (22)$$

where

$$S''(-P_1) = \left(\frac{\partial^2 S}{\partial p_z^2} \right)_{e, P=-P_1}$$

The numerical parameters Q and F are represented by the following integrals:

$$Q = \int_0^1 \frac{d\kappa}{\mathbf{K}(\kappa)} \left[\kappa(2\mathbf{E}(\kappa) - \mathbf{K}(\kappa))^2 + \frac{(\kappa^2\mathbf{K}(\kappa) + 2(\mathbf{E}(\kappa) - \mathbf{K}(\kappa)))^2}{\kappa^6} \right] = 0,32,$$

$$F = \int_0^1 d\kappa \left[\kappa(2\mathbf{E}(\kappa) - \mathbf{K}(\kappa)) \left(\frac{6\mathbf{E}(\kappa)}{\mathbf{K}(\kappa)} + 4\kappa^2 - 5 \right) + \frac{1}{\kappa^2} \left(\frac{2}{\kappa^2} - 1 + \frac{\pi^2}{\kappa^2\mathbf{K}^2(\kappa)} - 6 \frac{\mathbf{E}(\kappa)}{\kappa^2\mathbf{K}(\kappa)} \right) \left(\left(\frac{2}{\kappa^2} - 1 \right) \mathbf{K}(\kappa) - \frac{2}{\kappa^2} \mathbf{E}(\kappa) \right) \right] = 0,44.$$

The term proportional to μ will only be nonzero for a non-quadratic electron spectrum.

For a dispersion law $\varepsilon(\mathbf{p}) = \mathbf{p}^2/2m$, Eq. (22) becomes

$$\Delta\sigma = \sigma_0 \frac{12Q(q^2-1)^{1/2}\hbar^{1/2}}{\pi q^3}, \quad (23)$$

where $q = kv_F/\omega_c$; $q = 1$ corresponds to the collisionless cyclotron absorption threshold, while $\sigma_0 = en_0c/B_0$. According to Eq. (23) the conductivity shifts most severely at $q = (6/5)^{1/2}$, although it should be recalled that Eqs. (22) and (23) are only valid when

$$q-1 \gg q_0-1,$$

where q_0 corresponds to the bifurcation point (see Sec. 2 and Fig. 3b). In the case of an isotropic and a quadratic dispersion law, q_0 takes the form

$$q_0 = (1 + \hbar^2)^{1/2}.$$

It then follows from Eq. (22) as well as the parameters μ, η , and ν , that $\Delta\sigma$ is proportional to the square root of the dimensionless amplitude of the electromagnetic wave \hbar . In general this correction can be either positive or negative depending on the sign and the value of parameters μ and ν .

The nonlinear renormalization of cyclotron damping of electromagnetic waves determined by the dissipative component of the conductivity tensor σ_{xx} has been treated previously in Ref. 4. This study demonstrated that when

$$a = (\bar{\omega}\tau_p)^{-1} \ll 1$$

holds, implying that the collision frequency is much less than the oscillation frequency of the particles at resonance, the conductivity σ_{xx} and the absorption coefficient both decrease by a factor of approximately $2a$ compared to the linear case. Assuming $a \ll 1$, we calculate the nonlinear corrections to the spectrum [its real part $\omega(k)$] neglecting damping entirely. Using the resulting expression for the nonlinear correction to the conductivity (22) it is, in principle, possible to find the change in the wave vector Δk for a given frequency ω , which is consistent with experimental conditions. For this purpose we write the nonlinear dispersion equation as

$$\frac{(k+\Delta k)^2 c^2}{4\pi\omega} = \pm \sigma_{xy}(k+\Delta k, \hbar), \quad (24)$$

where

$$\sigma_{xy}(k, \hbar) = \sigma_{xy}^L(k) + \Delta\sigma(k),$$

the wave vector k in Eq. (24) is a solution of the linear dispersion equation

$$\frac{k^2 c^2}{4\pi\omega} = \pm \sigma_{xy}^L(k), \quad (25)$$

while Δk is the unknown nonlinear correction to the wave vector k ; the “+” and “-” signs represent the corresponding polarizations. Linearizing Eq. (24) with respect to Δk we have

$$\frac{\Delta k}{k} = \frac{\Delta\sigma(k)}{2\sigma_{xy}^L(k) - k \partial\sigma_{xy}^L(k)/\partial k}, \quad (26)$$

or, using relation (25),

$$\Delta k = \pm 4\pi \frac{v_p^2}{c^2 v_g} \Delta\sigma(k), \quad (27)$$

where $v_g = (d\omega/dk)_{\hbar=0}$ is the group velocity.

These expressions for the modification of the wave vector (26), (27) and the correction to the conductivity (22) provide a solution in principle to spectral renormalization when $\varepsilon(\mathbf{p})$ is known.

5. THE ANOMALOUS DOPPLERON

Fisher *et al.* first experimentally detected a dependence of the spectrum of electromagnetic waves in metal on their amplitude in cadmium.³ We know that electron (“-” polarization) and hole (“+” polarization) dopplersons exist in this compensated metal under linear conditions and that they propagate along the magnetic field lying on the C_6 axis. The electron dopplerson has a wave vector k less than ω_c/v_{\max} corresponding to the collisionless electron cyclotron absorption threshold, while the wave vector of the hole dopplerson is less than the cyclotron hole absorption threshold ($k \approx 3.77\omega_c/v_{\max}$).

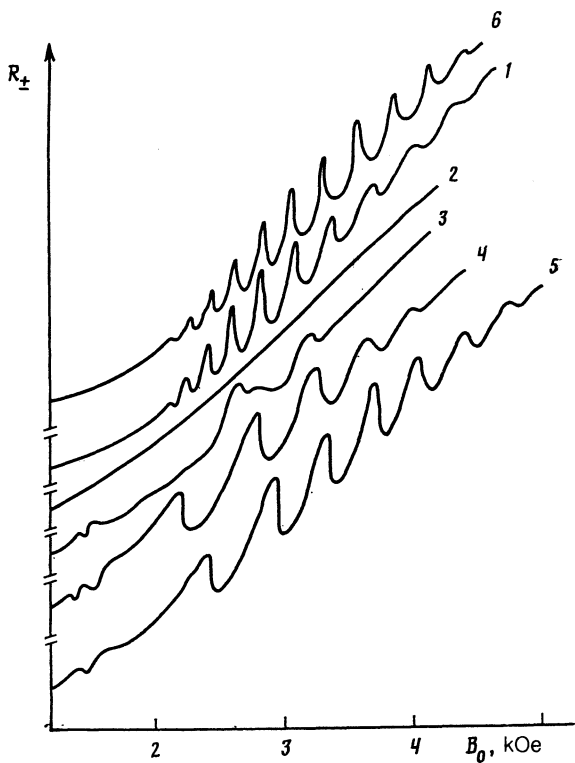


FIG. 4. Surface impedance oscillations of a cadmium wafer. Wafer thickness $d = 1.71$ mm, temperature = 4.2 K.

A new type of electromagnetic excitation of “+” polarization with a wave vector near the electron cyclotron absorption threshold was first detected experimentally in Ref. 3. This anomalous doppleron was only observed under nonlinear conditions at a dimensionless wave amplitude $h \gtrsim 10^{-2}$. Figure 4 shows the magnetic field dependence of the surface impedance of a cadmium wafer R_{\pm} (the plot was graciously provided to us by the authors of Ref. 3). Curves 1 and 6 correspond to “-” polarization and are plotted at alternating field amplitudes of 4 and 75 Oe, respectively, at 32 kHz. No nonlinearity of this polarization is observed in practice. This is a natural outcome since negatively polarized waves only exist in a near-threshold region containing no resonant electrons. Curves 2–5 correspond to “+” polarization and are plotted at the same frequency at amplitudes of 4, 40, 63, and 75 Oe, respectively.

The graphs clearly reveal that the nonlinearity primarily appears in oscillations in the surface impedance at a finite electrical wave amplitude, with the oscillations shifting towards stronger magnetic fields with increasing amplitude and the period of such oscillations decreasing. Figure 5 shows the period of the impedance oscillations ΔB plotted as a function of the external constant magnetic field B_0 . Curve 1 corresponds to a “-” doppleron. Curves 2 and 3 were obtained by measuring the oscillation periods in curves 5 and 4 of Fig. 4, respectively.

The experimental data in Figs. 4 and 5 can be explained by the theory of nonlinear renormalization of the real part of the spectrum $\omega(k)$ developed in this paper and by recalling the suppression of cyclotron damping in the field of a finite-amplitude wave. As suggested by the analysis in the preced-

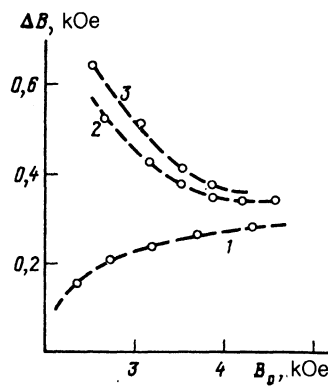


FIG. 5. Period of surface impedance oscillations vs the magnitude of the constant magnetic field.

ing section, a nonlinear correction to the nondissipative conductivity $\Delta\sigma$ will not radically alter the behavior of the conductivity and may produce a new “+” – polarized branch, an anomalous doppleron. Obviously, such a branch can be attributed to the nonlinear decrease in cyclotron damping (roughly by a factor of $2a$) beyond the absorption threshold. In order to test this conjecture we analyze a dispersion equation for “+” polarized waves (24) by writing the equation in dimensionless form

$$\xi_0^{-1} = \Phi(q). \quad (28)$$

Here

$$\xi_0 = 4\pi\omega n_0 c m^2 v_{\max}^2 / e B_0^3,$$

the parameter $q = kv_{\max} / \omega c$, v_{\max} is the maximum possible velocity of electrons in the metal in the direction of the magnetic field;

$$\Phi(q) = (1/q^2) (1 + \sigma_{xy}^e / \sigma_h),$$

where σ_{xy}^e is electron conductivity, while σ_h is hole conductivity equal to $en_0 c / B_0$ in the local limit (n_0 is concentration). In the dispersion equation (28) we have neglected entirely the dissipative part of the conductivity as well as the damping because they are proportional to the small parameter $2a$, which is of order 10^{-1} under experimental conditions.

The function $\Phi(q)$ will essentially depend on the behavior of the electron spectrum near the intersections with the external value of $\partial S / \partial p_z$. Assuming that the lens electrons in cadmium responsible for the conductivity singularity at the threshold have a spectrum

$$\varepsilon(p_{\perp}; p_z) = \frac{p_{\perp}^2}{2m} + v_0 |p_z| - \frac{bv_0}{n+1} (|p_z| - p_0)^{n+1},$$

$$n = 2, 4, 6, \dots, \quad (29)$$

where p_0 is the inflection point and $v_0 = v_z(p_0)$ is the maximum velocity (Fig. 1b), it is clearly evident that in the case of an elliptical reference point (we have such a situation for any n , for $p_F < p_0$; see Fig. 1a) the conductivity and its function $\Phi(q)$ are finite and continuous at the threshold (only the derivative $d\Phi/dq$ has a singularity), as demonstrated by

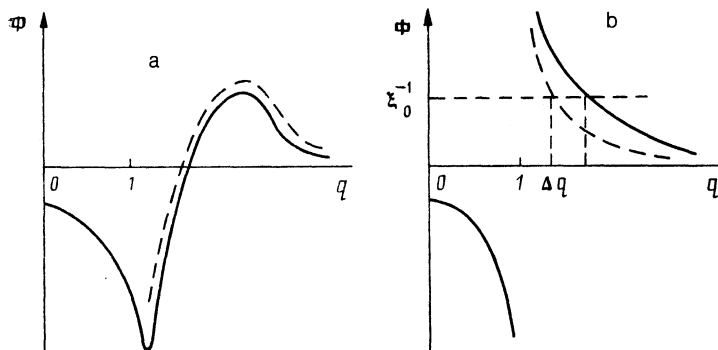


FIG. 6. The right side of the dispersion equation (28) for different electronic spectrum models under linear (solid curve) and nonlinear (dashed curves) conditions.

Fig. 6a. Qualitatively, the behavior of $\Phi(q)$ remains unchanged for $p_F \geq p_0$, if $n = 2$. However, the conductivity at the threshold in this case will tend logarithmically towards $-\infty$ on both sides of the threshold for $p_F = p_0$, while it also has a logarithmic singularity for $p_F > p_0$ with values of $q < 1$ and begins to appear at a certain finite negative value immediately beyond the threshold. For $p_F \geq p_0$, with $n \geq 4$, the function $\Phi(q)$ behaves as shown in Fig. 6b, i.e., it decays monotonically everywhere for $q > 1$. It is possible to obtain a graphical “+” solution for $q > 1$ (the anomalous doppleron) as the intersection of the curve $\Phi(q)$ with the constant $\xi_0^{-1}(B_0)$.

Which of these $\Phi(q)$ relations can explain the experimental results? An answer to this question can be found by analyzing the curves shown in Figs. 4 and 5. The period of the impedance oscillations of the wafer $\Delta B(B_0)$ in a constant magnetic field is given by the following expression (see Ref. 5):

$$\Delta B = \frac{\Delta B_{G-K}}{q + 3\Phi(q)dq/d\Phi}, \quad (30)$$

where ΔB_{G-K} is the period of the Gantmakher-Kaner oscillations, while $q(B_0)$ is the solution of the dispersion equation (28). The plot of $\Delta B(B_0)$ in Fig. 5 clearly shows that the period of oscillations of the anomalous doppleron will always exceed ΔB_{G-K} and will asymptotically approach this value with increasing magnetic field B_0 . According to Eq. (30) this reveals that the derivative $d\Phi/dq$ must be negative in the range of the “+” doppleron. Such ranges are found in both Fig. 6a and 6b. However, the oscillation period does not tend toward ΔB_{G-K} for the conductivity shown in Fig. 6a in strong magnetic fields with values near the upper critical field. The relation $\Delta B(B_0)$ for the case shown in Fig. 6b will, according to Eq. (30), correspond to experiment.

We now discuss the nonlinear renormalization effects of the real part of the spectrum. Such effects are manifested, first, as a decrease in the oscillation period, as shown in Fig. 5 (curves 2 and 3) and, second, as a shift in the oscillation peaks towards stronger magnetic fields as the amplitude of the alternating field increases.

Analysis of such effects requires a consideration of the nonlinear correction to the function $\Phi(q)$, which is equal to

$$\Delta\Phi(q) = \frac{1}{q^2} \frac{\Delta\sigma}{\sigma_h},$$

where $\Delta\sigma$ can be calculated by means of Eqs. (22) and (9).

When the electronic spectrum is described by Eq. (29) this correction takes the form

$$\Delta\Phi = -\frac{64mv_0p_0^2}{(2\pi\hbar)^2 n_0 b n q_1^2} \left(\frac{\hbar}{nb}\right)^{1/2} \left(\frac{2mv_0}{p_0}\right)^{1/2} \left(\frac{b}{q_1-1}\right)^{(2n-7)/4n} \times \left(1 + \alpha \left(\frac{b}{q_1-1}\right)^{1/n}\right)^{1/2} \left[\frac{F}{3}(n-1) \left(1 + \alpha \left(\frac{b}{q_1-1}\right)^{1/n}\right) - \frac{Q}{2}\right], \quad (31)$$

where q_1 is the dimensionless wave vector defined by the condition $q_1 = kv_0/\omega_c$, while $\alpha = (p_F - p_0)/p_0$. For $p_F \geq p_0$ the parameter q_1 is identical to the parameter q introduced above. If, on the other hand, we have $p_F < p_0$, their relation is given by $q_1 = q(1 + b\alpha^n)$.

We now discuss the behavior of the correction $\Delta\Phi$ for different spectral models. For $n = 2$ the characteristic behavior of the renormalized function $\Phi(q)$ is shown in Fig. 6a: the correction is everywhere positive and drops off precipitously to zero for $q \gg 1$. In practice this result does not depend on the relation between p_F and p_0 , although there may be a sign reversal of $\Delta\Phi$ for $p_F < p_0$. The renormalized function $\Phi(q)$ is shown in Fig. 6b for $n = 4$. The nonlinearity always gives rise to a reduction in conductivity and moderation of the singularity at the cyclotron absorption threshold. This is perfectly understandable behavior, since the nonlinear distribution function, unlike the linear distribution function, has no singularities.

It is possible to provide a qualitative explanation for the experimental results of Ref. 3 if we assume that the cadmium conductivity beyond the collisionless cyclotron absorption threshold behaves as shown in Fig. 6b. In this case, the effects discussed above—the shift in oscillation frequency and the reduction of the period ΔB with increasing wave amplitude—have the correct sign and are of the same order of magnitude. To test this assumption, proceeding from the condition

$$k(B_0; \hbar)d = 2\pi n,$$

which indicates that n wavelengths are accumulated in a metallic wafer of thickness d , we obtain an expression for the shift of the n th oscillation as the amplitude goes from h_1 to h_2 :

$$\delta B_0 = \frac{\Delta k(h_1) - \Delta k(h_2)}{(dk/dB_0)_{h=0}},$$

where $\Delta k(h)$ is given by Eq. (26). Then, using the relation between the wave vector k and the dimensionless parameter q , this expression can be written as

$$\delta B_0/B_0 = \frac{\Delta B}{\Delta B_{G-K}} (\Delta q(h_1) - \Delta q(h_2)), \quad (32)$$

where $\Delta q = q\Delta k/k$. Equation (32) gives the correct direction of the shift and its relative order of magnitude 10^{-1} for the first oscillations shown in Fig. 4 as the amplitude rises from 63 to 75 Oe (curves 4 and 5), which is in qualitative agreement with experiment. The ratio $\Delta B/\Delta B_{G-K}$ in this case can be directly determined from the curves shown in Fig. 5. The sign on δB_0 is not identical to the experimentally derived value for the case corresponding to Fig. 6a.

The decrease in oscillation period with increasing wave amplitude can be described by Eq. (20), which is more conveniently written as

$$\Delta B = \frac{\Delta B_{G-K}}{(mc v_0/e)(dk(B_0;h)/dB_0)}. \quad (33)$$

The derivative $dk(B_0;h)/dB_0$ grows with increasing amplitude, a can easily be verified by plotting $k(B_0)$ from the known relation $\Phi(q)$ (Fig. 6b). A rough estimate of the magnitude of variation in the period as the amplitude rises from h_1 to h_2 can be obtained by writing the difference of the periods as

$$\frac{\Delta B(h_1) - \Delta B(h_2)}{\Delta B(h_1)} \sim \frac{d}{dB_0} [B_0(\Delta q(h_1) - \Delta q(h_2))] \sim h_2^{1/2} - h_1^{1/2}. \quad (34)$$

An estimate using Eq. (34) for curves 4 and 5 in Fig. 4 yields the same order of magnitude of the effect as experiment.

This theory of nonlinear spectral renormalization of electromagnetic waves in metals therefore explains the nature of the anomalous doppleron in cadmium, as well as its fundamental properties; the theory reveals that these effects depend strongly on the form of the electronic spectrum of the metal.

It is worth noting in closing that one of the effects accompanying nonlinear spectral renormalization is a modulational instability that leads to a smooth, periodic dependence of wave amplitude on the coordinate. The modulational instability, however, only manifests itself if the modulation period is far smaller than the characteristic damping length of the wave. It is not likely that this condition holds in the experiment described in Ref. 3, and hence the modulational instability effects were not examined in the present paper.

The authors wish to express their sincere gratitude to L. M. Fisher for extensive, useful advice and critical commentary. We also thank I. F. Voloshin, A. S. Chernov, and N. A. Podlevskii for fruitful discussions.

APPENDIX

By means of the generating function

$$F_2 = (kz - \omega t)P_\xi$$

we introduce into the Hamiltonian (6) a new variable $\xi = kz - \omega t$ and its conjugate momentum $P_\xi = p_z/k$. This canonical transform is equivalent to a transformation to a frame that is comoving with the phase velocity of the wave along the magnetic field \mathbf{B}_0 . Hamiltonian (6), after the canonical transform, is written as

$$H = \varepsilon(p_\perp(p_x, x, \xi); kP_\xi) - \omega P_\xi \quad (A1)$$

and is the integral of motion.

The subsequent analysis of the electron dynamics differs from our analysis carried out in Sec. 2 for the simple spectral model (1). Canonical variables $\{I, \varphi\}$ and $\{P_\xi, \xi\}$ are conveniently used to reduce the equations of motion to a one-dimensional system similar to Eq. (3). This can be carried out by means of a generating function of the type

$$F_2 = \xi P_\xi + \int p_x(I, x, \xi) dx,$$

where the action I is proportional to the area $S(\varepsilon, p_z)$ of the electron orbit in momentum space in a uniform magnetic field:

$$I = \frac{c}{2\pi e B_0} S(\varepsilon, P_\xi) = \frac{c}{2e B_0} p_\perp^2. \quad (A2)$$

The phases φ and ξ are expressed through the new action and the old coordinates as

$$\varphi = \frac{\partial F_2}{\partial I} = \arcsin \frac{x + x_0 + (h/k) \cos \xi}{(2cI/eB_0)^{1/2}},$$

$$\xi = \frac{\partial F_2}{\partial P_\xi} = \xi.$$

The relation between the momentum P_ξ and the new momentum P_ξ is given by

$$P_\xi = \frac{\partial F_2}{\partial \xi} = P_\xi - \frac{h}{k} \left(\frac{2eB_0}{c} I \right)^{1/2} \sin(\xi + \varphi).$$

Now writing the Hamiltonian (A1) in the new variables we have

$$H = \varepsilon \left(I, kP_\xi - h \left(\frac{2eB_0}{c} I \right)^{1/2} \sin(\xi + \varphi) \right) - \omega P_\xi + h v_p \left(\frac{2eB_0}{c} I \right)^{1/2} \sin(\xi + \varphi).$$

Finally, since the Hamiltonian function depends only on the sum of the phases, we introduce the variable $\beta = \xi + \varphi + \pi/2$ and the conjugate action J :

$$F_2 = (\xi + \varphi + \pi/2)P + J\varphi,$$

which yields

$$\varphi = \varphi, \quad I = P + J, \quad (A3)$$

$$\beta = \xi + \varphi + \pi/2, \quad P_\xi = P.$$

The Hamiltonian then takes the form

$$H = \varepsilon \left(J + P; kP + h \left(\frac{2eB_0}{c} (J + P) \right)^{1/2} \cos \beta \right) - \omega P - h v_p \left(\frac{2eB_0}{c} (J + P) \right)^{1/2} \cos \beta. \quad (A4)$$

The Hamiltonian function is independent of the variable ϑ , as follows from Eq. (A4), and hence the action J is an integral of motion.

The phase velocity of the wave v_p is commonly much less than the characteristic electron velocity in metals. We ignore the last two terms proportional to ω and v_p in (A4) in order to avoid complicating the subsequent calculation. In

the remaining term we carry out an expansion to second order in the small parameter $h \ll 1$. Finally we have for the Hamiltonian and the equations of motion

$$H = \varepsilon(J+P; P) + hv_z \left(\frac{2eB_0}{c} (J+P) \right)^{1/2} \cos \beta, \quad (\text{A5})$$

$$\dot{\beta} = kv_z + \omega_c + h \frac{\partial}{\partial P} (v_z p_{\perp})_J \cos \beta, \quad \dot{P} = hv_z p_{\perp} \sin \beta, \quad (\text{A6})$$

where the transverse momentum is

$$p_{\perp} = \left(\frac{2eB_0}{c} (J+P) \right)^{1/2},$$

while the subscript J denotes that the partial derivative is taken with a fixed value of J .

¹G. J. Morales and T. M. O'Neil, Phys. Rev Lett. **28**, 417 (1972).

²V. I. Karpman and B. V. Lindin, Zh. Eksp. Teor. Fiz. **70**, 1278 (1976) [Sov. Phys. JETP **43**, 666 (1976)].

³I. F. Volomin, N. A. Podlevskikh, V. G. Skobov *et al.*, Zh. Eksp. Teor. Fiz. **94**, 322 (1988) [Sov. Phys. JETP **67**, 613 (1988)].

⁴I. F. Volomin, G. A. Vugal'ter, V. Ya. Demikhovskiy *et al.*, Zh. Eksp. Teor. Fiz. **73**, 1503 (1977) [Sov. Phys. JETP **50**, (1977)].

⁵O. V. Konstantikov, V. G. Skobov, V. V. Lavrova *et al.*, Zh. Eksp. Teor. Fiz. **63**, 224 (1972) [Sov. Phys. JETP **36**, 118 (1972)].

Translated by Kevin S. Hendzel